MINIMIZING BEAM MOTION IN A LONG-PULSE LINEAR INDUCTION ACCELERATOR*

Carl Ekdahl#, E. O. Abeyta, J. B. Johnson, K. Nielsen, M. E. Schulze,
LANL, Los Alamos, NM 87545, U. S. A.
C.-Y. Tom, NSTec, Los Alamos, NM 87545, U. S. A.
T. P. Hughes, C. H. Thoma, Voss Scientific, Albuquerque, NM 87108, U. S. A.

Abstract

The Dual Axis Radiography for Hydrodynamic Testing (DARHT) Facility at Los Alamos uses two linear induction accelerators (LIAs) for flash radiography of explosively driven experiments from orthogonal viewpoints. The DARHT Axis-II long-pulse 1.8-kA, 16.5-MeV LIA is unique. It has a beam pulse with a 1.6-μs current flattop during which the kinetic energy varies by less than ± 2%. During this flattop, a kicker cleaves out four short micro-pulses, which are focused onto a high-Z target and converted to bremsstrahlung for multi-pulse flash radiography of the experiments.

Asymmetric injection of the beam into the solenoidal focusing field, small temporal variations in accelerating potentials, and slight cell misalignments combine to cause the beam position to wander during the flattop. This is undesirable for radiography. The slow beam motion in the LIA causes a displacement of the four radiographic source spots. Moreover, since the specific energy deposition from each micro-pulse is sufficient to vaporize target material, succeeding pulses impact an asymmetric object causing a distortion of the source spot. Therefore, we have spent some effort to tune out the beam motion at the exit of the LIA.

INTRODUCTION

The Dual-Axis Radiography for Hydrodynamic Testing (DARHT) facility produces flash radiographs of explosive hydrodynamic experiments. Two linear induction accelerators (LIAs) make the bremsstrahlung radiographic source spots for orthogonal views of each test. The 2-kA, 20-MeV Axis-I LIA creates a single 60-ns radiography pulse. The 1.8-kA, 16.5-MeV Axis-II LIA creates up to four radiography pulses by kicking them out of a longer pulse that has a 1.6-μs flattop (Fig. 1). Both accelerators produce radiographic source spots with full width at half-maximum (FWHM) < 1 mm.

The long-pulse Axis-II LIA, the beam it produces and accelerates, simulations, and diagnostics are described in Ref. [1- 3]. The kicker and downstream transport (DST) to the bremsstrahlung converter are described in Ref. [4]. Figure 1 shows the long pulse accelerated by the Axis-II LIA and the shorter kicked pulses for one of many possible kicker formats.

*Work supported by the US National Nuclear Security Agency and the US Department of Energy under contract W-7405-ENG-36.
#cekdahl@lanl.gov

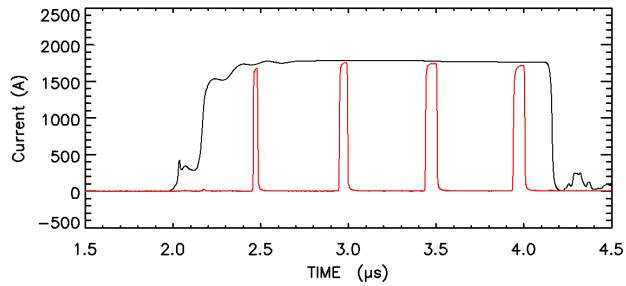

Figure 1: Overlay of current at LIA exit (black) and after the kicker (red) showing the long accelerated-current pulse and four kicked-current pulses.

High-frequency beam motion, with period less than a kicked pulsewidth, would increase the radiographic source spot size, which is integrated over the pulsewidth.

Low frequency beam motion, with a period greater than the kicked pulse FWHM, would result in displacement of successive radiographic source spots, and in possible distortion of the later spots from asymmetric target erosion.

Therefore, we make an effort to minimize both high- and low- frequency motion in our LIA.

High-Frequency Motion – BBU

BBU frequencies in this LIA range from ~120-MHz up to ~600-MHz. We suppress BBU by incorporating ferrite tiles in the cells to damp the modes, and by using strong focusing fields [3, 6]. The remaining BBU measured with the beam position monitor (BPM) at the accelerator exit is less than 2% of the beam radius (Fig. 2).

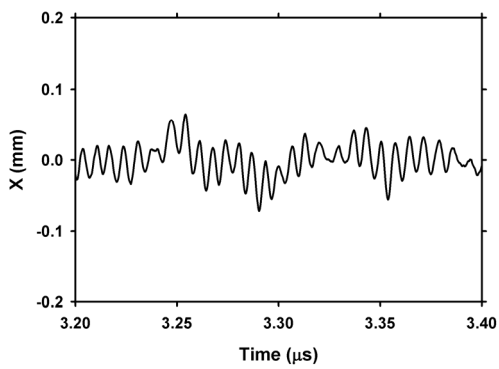

Figure 2: BPM measurement of BBU motion at accelerator exit, which is < 2% of .the ~5-mm beam radius calculated by our envelope codes.

Low-Frequency Motion – Ion Hose Instability

Figure 2 also shows evidence of low-frequency, ~17-MHz motion with about the same amplitude as the BBU. This is in the frequency range of the ion-hose instability in low pressure air [3]. Even though our background pressure is less than 1.0E-7 Torr, theory and previous experiments imply that we should still have some slight residual instability [3]. Like the BBU, it is suppressed to less than 2% of the beam radius by the strong solenoidal focusing field.

Low-Frequency Motion – Beam Sweep

Beam motion during the flattop was originally dominated by an energy dependent sweep, with > 5 mm amplitude at the LIA exit. The source of this sweep was an initially large helical trajectory through the accelerator (Fig. 3) caused by asymmetric beam injection due to the folded current path in the diode [5].

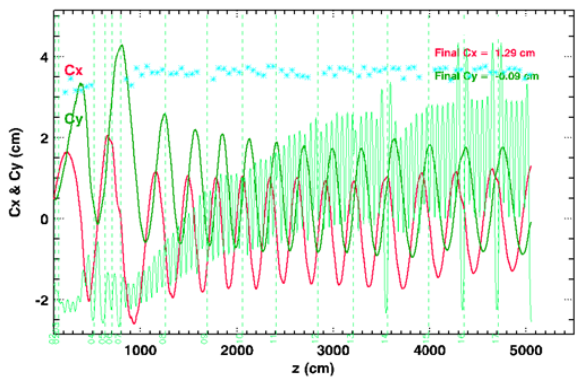

Figure 3: Simulation of uncorrected beam centroid position in x (Cx in red) and y (Cy in green). The solenoidal focussing field strength on axis is also shown in green, as are the accelerating potentials in blue.

The gyro-radius and phase of the helical trajectory at any point in the LIA depend on the beam energy. For constant accelerating potentials, the beam position at the exit would be fixed. However, the accelerating cell potentials actually vary in time, resulting in the final energy variation shown in Fig. 4. This causes the beam position to wander around the flux tube enclosed by the helix. Figure 5 shows simulations of how the beam position at the LIA exit varies as a function of the accelerating potential variation.

We reduce the sweep by first correcting for the asymmetric injection using dipole correctors in the injector cells (Fig. 6). However, even after correcting this initial offset, the beam is deflected into a helical trajectory by the dipoles resulting from small cell misalignments. Again, beam energy variation causes motion of the beam position at the LIA exit as in Fig. 5, albeit about a smaller helix. This is the "corkscrew" motion observed in other LIAs, and it can be significantly reduced by using corrector dipoles in a procedure called a "tuning V" [7,8].

With only minor correction for the asymmetric injection, and no tuning V corrections for misalignment, this beam energy variation causes the beam at the exit to sweep around a ~3.5-mm radius helix during the flattop time window (Fig.4). This uncorrected sweep is shown in Fig. 7.

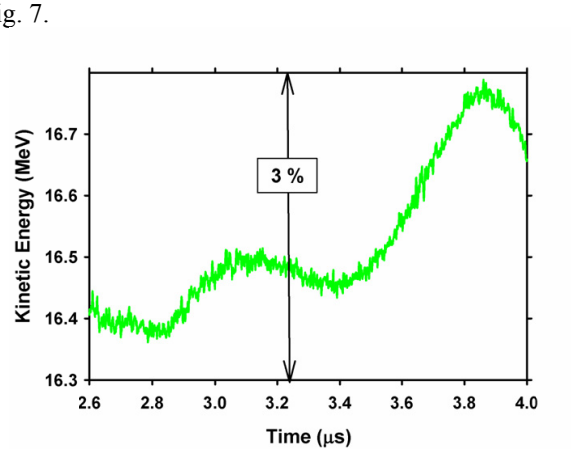

Figure 4: Beam kinetic energy measured at the LIA exit during the flattop (Fig. 1).

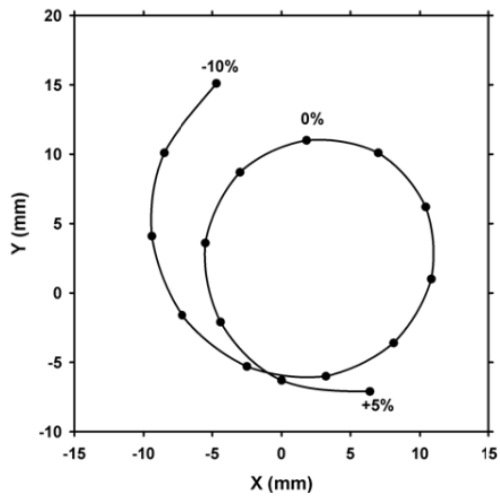

Figure 5: Simulation of beam position at LIA exit resulting from coherent % variation of the accelerator cell potentials. If the cell potentials vary with time, the beam position moves around the flux tube as shown.

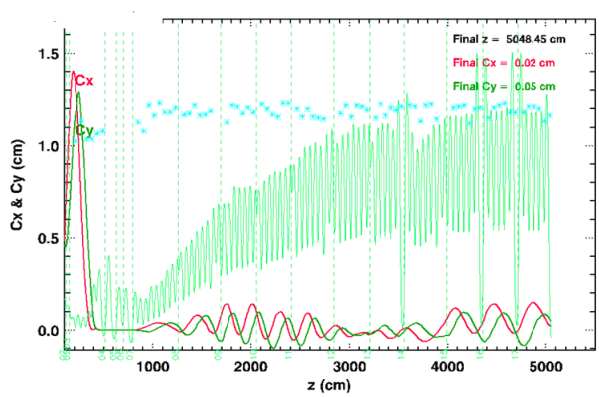

Figure 6: For this simulation initial large helical motion resulting from asymmetric injection has been corrected using dipoles in the six injector cells. The residual helical motion is the result of cell misalignments.

Accurate centering of the beam out of the injector as shown in Fig. 6, along with applications of the tuning V procedure at two locations, significantly reduced the sweep (Fig. 8). Using the diagonal of the bounding rectangle as a measure of sweep, we reduced this to ~1.2 mm during the 1.4-μs window of the energy variation shown in Fig. 4. This is a significant reduction of the uncorrected value of more than 5 mm (Fig. 7).

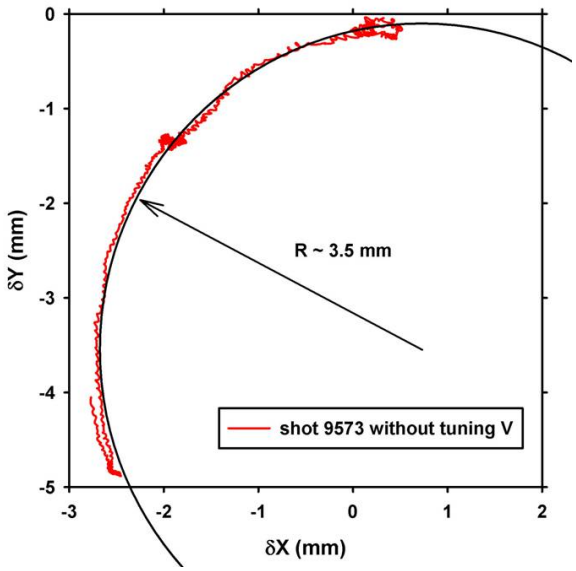

Figure 7: Motion of beam caused by the ~2.5% energy variation shown in Fig. 4. The ~120 degree sweep is close to simulation predictions (Fig. 5).

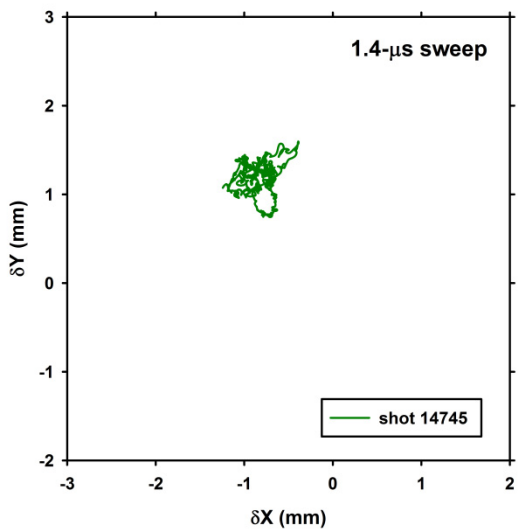

Figure 8: Reduction of sweep by centering the beam out of the injector and using the "tuning V" procedure [7,8]. (Compare with Fig. 7.)

Including the first pulse, which is slightly ahead of the flattop (Fig. 1), the sweep is ~1.6 mm at the times of the four radiographs. Since this is ~32% of the ~5-mm predicted radius at that location, the first-to-last displacement of the radiographic source spots at the final focus is expected to be less than 25% of the source spot FWHM.

CONCLUSIONS

We have suppressed beam motion in the Axis-II LIA to amplitudes small enough to have little effect on radiographic performance. The solenoidal magnetic focusing field was strong enough to suppress the BBU and ion-hose instabilities to less ~2% of the beam radius. Low-frequency beam sweep was reduced to less than 1/3 of the beam radius during the radiographic pulse train, so the resulting displacement of source spots should be less than 50% of the spot FWHM. Future efforts to further reduce the sweep will include varying the timing of the cell pulsed power to minimize the kinetic energy variation, which is one source of the problem.

REFERENCES

[1] Carl Ekdahl, et al., "First beam at DARHT-II," in Proc. 2003 Part. Accel. Conf. (2003), pp. 558-562.
[2] Carl Ekdahl, et al., "Initial electron-beam results from the DARHT-II linear induction accelerator," IEEE Trans. Plasma Sci. 33 (2005), pp. 892-900.
[3] Carl Ekdahl, et al., "Long-pulse beam stability experiments on the DARHT-II linear induction accelerator," IEEE Trans. Plasma Sci. 34 (2006) pp.460-466.
[4] Martin Schulze, et al., "Commissioning the DARHT-II Accelerator Downstream Transport and Target," in Proc. 2008 Linear Accel. Conf. (2008) pp. 427-429.
[5] T. P. Hughes, R. E. Clark, and S. S. Yu, "Three-dimensional calculations for a 4 kA, 3.5 MV, 2 microsecond injector with asymmetric power feed," Phys. Rev. ST Accel. Beams 2 (1999) pp. 110401-1 – 110401-6.
[6] Carl Ekdahl,et al., "Electron beam dynamics in the long-pulse, high-current DARHT-II linear induction accelerator," in Proc. 2009 Particle Accelerator Conf. (2009) pp. 3080-3084.
[7] Y.-J. Chen, "Control of transverse motion caused by chromatic aberration and misalignments in linear accelerators," Nucl. Instr. and Meth. in Phys. Res. A 398 (1997)pp.139-146.
[8] J. T. Weir, J. K. Boyd, Y.-J. Chen, J. C. Clark, D. L. Lager, and A. C. Paul, "Improved ETA-II accelerator performance," in Proc. 1999 Particle Accelerator Conf. (1999) pp. 3513-3515.